

Mechanical Behavior of a 9.7 MW Induction Motor Under Fault Conditions – A Case History

G. Richard Thomas, P.E.
Global Services Manager
RoMaDyn
1711 Orbit Way
Minden, NV USA

(775) 783-4642 (office)
(775) 783-4650 (cell)

richard.thomas@romadyn.com

ABSTRACT

By applying to the rotor system a known mass, at a known radius, a known centrifugal force is created at rotative speed, Ω . The science, and art, of field balancing involves the creation of a centrifugal force, at the correct angular location, so as to create a synchronous (1X) vibration response equal in magnitude but opposite to the direction of the 1X vibration vector that exists due to the residual unbalance in the rotor system.

By definition, field balancing is a form of synchronous perturbation. From the data obtained during field balancing, the influence vector, \vec{H} , may be calculated. The influence vector is defined for a specific set of operating conditions, e.g. operating speed, load, temperature, etc. Also, the influence vector, H , is inversely related to the synchronous dynamic stiffness, \vec{K}_{DS} , of the rotor system.

Therefore, calculating \vec{H} allows one to make an evaluation of K_{DS} for a given set of operating conditions. Changes in K_{DS} result from physical changes in one or more of the basic characteristics of the rotor system, e.g. modal spring stiffness, K ; modal damping D ; modal mass, M ; average circumferential velocity ratio, λ ; and rotative speed, Ω .

Synchronous, 1X, response, is equal to the centrifugal force acting on the rotor system due to the effective residual unbalance divided by \vec{K}_{DS} . Therefore, if the synchronous 1X vibration response increases it does so either due to: 1) an increase in the synchronous forcing

function, 2) a decrease in the synchronous dynamic stiffness, K_{DS} , or 3) both.

Over an 11 week period a 9.7 MW (13,000 Hp) induction motor driving a centrifugal compressor through a speed increaser gearbox was field balanced on *six different occasions* in order to maintain acceptable 1X vibration levels at operating speed. The need for subsequent balance attempts beyond the first correction clearly indicated that an abnormal situation existed where either the synchronous forcing function was increasing vs. time; the synchronous dynamic stiffness was decreasing vs. time; or both. This paper documents the analytical methodologies utilized in order to differentiate the root cause of the increase in the 1X vibration response over the 11 week period and final corrective action taken to remedy the situation.

INTRODUCTION

Fluid Catalytic Cracking (FCC) is the most common catalytic cracking process, in which the oil is cracked in the presence of powdered catalyst which is maintained in an aerated or fluidized state by the oil vapors passing through the catalyst.

The catalyst section contains the reactor, riser and regenerator, which forms the catalyst circulation unit. The catalyst is continuously circulated between the reactor and the regenerator using air, oil vapors, and steam as the conveying media. The preheated oil enters the bottom of the vertical reaction riser where it is mixed with hot regenerated catalyst. The hot catalyst vaporizes the oil and the vapor carries the powdered catalyst up the riser into the

reactor where the catalyst settles as a dense bed of whirling powder. The cracking reactions start in the riser and continue in the reactor bed; in the more modern FCC units, all cracking takes place in the riser. The cracking reactions take only a few seconds to complete, after which the catalyst particles must be separated from the fluid by the cyclone separators inside the reactors.

The spent catalyst contains coke, deposited on the particle surface during cracking, which must be removed. In the regenerator, the spent catalyst is mixed with an air stream from the main air blower and the coke is oxidized primarily into carbon monoxide. The cleaned catalyst is then reused.

The carbon monoxide exiting the regenerator is mixed with some very fine catalyst particles which are removed in another cyclone separator. The carbon monoxide then flows through a low pressure expander turbine which drives the main air blower, one of two major pieces of rotating machinery in a FCC unit. The blower is usually a low pressure ratio, high volume, single case centrifugal compressor which provides air to the regenerator. At full power the expander turbine is capable of driving the main air blower with the excess horsepower directed to a motor/generator. The carbon monoxide exiting the expander is burned in the preheat furnace to supplement the primary gas fired burners.

The fractionator separates product from the cracking process. Gas exiting the top of the fractionator column and the overhead drum is compressed and sent to the gas plant by the Wet Gas Compressor Train, the second major piece of rotating equipment in a FCC unit.

This case history involves the 9.7 MW motor drive for the Wet Gas Compressor Train in a major oil refinery located in the USA. The Wet Gas Compressor Train consists of the motor, a speed increasing gearbox, and a multistage centrifugal compressor. In late April, the refinery took a short maintenance outage in order to replace the motor drive for the Wet Gas Compressor Train.

NOMENCLATURE

\vec{C} : calibration response vector; $mil\ pp\ \angle\ \Phi^\circ$

\vec{W} : ⁱ "weight add vector"; $gram\ \angle\ \Theta^\circ$

$\vec{H}_{m,c}$: influence vector; $\frac{C}{W} \frac{mil\ pp}{gram} \angle \frac{\Phi^\circ}{\Theta^\circ}$

\vec{K}_{DS} : synchronous dynamic stiffness; $\frac{lb_f}{in} \angle -\frac{\Theta^\circ}{\Phi^\circ}$

MOTOR DESIGN

The motor is a custom engineered, high efficiency, wound rotor, induction motor designed for the specific application of driving the Wet Gas Compressor Train.

The motor rating is:

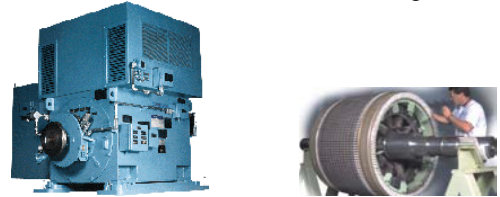
- 9.7 MW (13,000 hp)
- 13,200 volts / 30 Hz (1800 rpm)

Wound rotor motors are an extremely versatile breed of induction motors. Featuring a rugged design, these machines provide the unique ability to gradually bring up to speed high-inertia equipment and large loads smoothly and easily. Wound rotor motors also can develop high starting torque at standstill with minimum inrush current.

Long motor life is ensured with the use of external resistor banks or liquid rheostats that dissipate heat build-up generated during motor start-up.

What makes the wound rotor motor a unique induction machine is its rotor. Instead of a series of rotor bars, a set of insulated rotor coils is used. The rotor windings are similar to those found on a DC armature, with the coils connected together to a set of rings that make contact with carbon-composite brushes..

This rotor construction design allows for a varying resistance from almost short-circuit condition to an open-circuit condition with infinite external resistance. By modifying the resistance, the speed-torque characteristics can be altered. This allows for the torque to remain high, the inrush current to remain low, and the speed varied.



FIELD BALANCING: APRIL – JULY

Viewing the machine train from the outboard end of the motor, looking toward the compressor, motor rotation is Y to X (CW). Each motor bearing is monitored with permanently installed shaft observing proximity transducers, mounted at 45L (vertical) and 45R (horizontal) from top dead center (TDC). A permanently installed Keyphasor[®] transducer, mounted at TDC on the outboard end of the motor, observes a once per turn notch machined into the motor shaft. This Keyphasor[®] signal provided the reference for all phase information acquired during this project.

A part of the commissioning process for the newly installed motor was to trim balance the unit in the field. In situ field balancing was accomplished on Saturday, 27 April. Please refer to the data indicated by the blue arrow in Table 1 below.

Seven weeks later, on Friday, 14 June, the Wet Gas Compressor Train was shut down due to high motor IX vibration readings. Notice the difference between the final balance condition on 27 April and the initial balance condition on 14 June as indicated by the red arrows in Tables 1 and 2 below.

i NOTE: In the various reference materials, it has become the accepted practice to refer to the addition of or removal of **mass** from the rotor as a *weight* change. This is incorrect and often leads to confusion.

Mass and force terms do not have the same units. The term weight means force. One does not directly add or remove “force” from the rotor.

During balancing, mass is either added to or removed from the rotating assembly at a defined radius. The resulting **centrifugal force** is the product of **mass**, **balance radius**, and **rotative speed squared**.

In order to minimize confusion, in this presentation, the conventional use of *balance weight* will be utilized. However, it is very important to remember that this is a colloquialism and is incorrect. Proper engineering units must be utilized in all calculations.

Balance Summary Data: April 27 - July 14, 2005														
Run No.	Data Type	Date	Day of the Week	Elapsed Time	Speed (rpm)	BP	Mass Added (gms)	Mass Angle	+	-	Outboard 45L (vertical xducer) (mil pp @ Φ)	Outboard 45R (horz xducer) (mil pp @ Φ)	Inboard 45L (vertical xducer) (mil pp @ Φ)	Inboard 45R (horz xducer) (mil pp @ Φ)
1	Initial	27-Apr-05	Wed	0 Days	1792	1	118	300°	+		2.90 @ 225°	0.70 @ 346°	3.80 @ 211°	1.90 @ 325°
	Final	27-Apr-05				2	118	300°	+		0.30 @ 4°	0.50 @ 99°	0.60 @ 151°	0.40 @ 307°
2	Initial	14-Jun-05	Tues	48 Days	1792	1	130	15°	+		4.17 @ 313°	1.84 @ 69°	4.16 @ 302°	2.08 @ 46°
	Final	14-Jun-05				2	130	15°	+		0.52 @ 340°	0.44 @ 106°	0.56 @ 234°	0.72 @ 338°
3	Initial	21-Jun-05	Tues	7 Days	1792	1	150	0°	+		4.32 @ 289°	1.98 @ 42°	3.77 @ 280°	2.10 @ 39°
	Final	21-Jun-05				2	150	0°	+		0.88 @ 137°	0.22 @ 212°	1.44 @ 165°	1.36 @ 293°
4	Initial	28-Jun-05	Tues	7 Days	1792	1	179	330°	+		4.50 @ 269°	1.36 @ 15°	5.07 @ 258°	2.50 @ 350°
	Final	28-Jun-05				2	179	330°	+		1.11 @ 72°	0.51 @ 182°	1.14 @ 113°	1.26 @ 263°
5	Initial	5-Jul-05	Tues	7 Days	1792	1	159	345°	+		3.86 @ 281°	1.19 @ 22°	4.10 @ 266°	1.93 @ 345°
	Final	5-Jul-05				2	159	345°	+		0.73 @ 184°	0.45 @ 182°	1.69 @ 178°	1.93 @ 190°
6	Initial	14-Jul-05	Wed	9 Days	1792	1	160	315°	+		3.23 @ 240°	1.25 @ 334°	3.85 @ 224°	2.39 @ 315°
	Final	14-Jul-05				2	160	315°	+		0.79 @ 123°	0.60 @ 245°	1.49 @ 149°	2.02 @ 268°

Notes:

- 1) BP = Balance Plane; 1=Outboard; 2= Inboard
- 2) The "+" sign = mass added
- 3) The "-" sign = mass removed
- 4) All vibration data is shaft relative displacement data
- 5) Mass added at a 12.5 inch balance radius
- 6) Mass angle is referenced to the 45L (vertical) transducer with the Keyphasor transducer aligned with the once per turn hole.
- 7) Rotor rotation is CW as viewed from the outboard end

TABLE 1

CHANGE IN 1X VIBRATION VECTOR vs TIME					
From	To	Outboard 45L (vertical xducer) (mil pp @ Φ)	Outboard 45R (horz xducer) (mil pp @ Φ)	Inboard 45L (vertical xducer) (mil pp @ Φ)	Inboard 45R (horz xducer) (mil pp @ Φ)
27-Apr-05	14-Jun-05	3.99 @ 310°	1.43 @ 59°	4.69 @ 306°	2.18 @ 56°
14-Jun-05	21-Jun-05	4.01 @ 283°	1.83 @ 30°	3.40 @ 287°	1.86 @ 59°
21-Jun-05	28-Jun-05	5.13 @ 276°	1.57 @ 17°	5.34 @ 274°	2.10 @ 23°
28-Jun-05	5-Jul-05	4.86 @ 275°	1.68 @ 16°	5.14 @ 272°	2.15 @ 20°
5-Jul-05	14-Jul-05	2.89 @ 252°	1.66 @ 341°	2.94 @ 248°	3.84 @ 339°
TOTAL 1X VECTOR CHANGE vs TIME					
27-Apr-05	14-Jul-05	19.97 @ 280°	7.45 @ 20°	11.20 @ 294°	10.35 @ 20°

TABLE 2

Tables 1 and 2 summarize the initial and final 1X vibration data as the motor rotor was field balanced on six separate occasions, e.g. 27 April, 14 June, 21 June, 28 June, 5 July, and 14 July. Over this eleven week period, an equivalent of 715.5 grams @ 0° (\vec{W}) was added to **each** end of the rotor at a fixed radius of 12.5 inches. At an operating speed of 1792 rpm, this equates to a total, equivalent, applied centrifugal force of 3,590 lb_f, or 0.855g (rotor first mode modal mass \Rightarrow 4,200 lb_m).

It must be emphasized that repetitive balancing of a rotor coupled with the addition of large amounts of mass are well outside of the norm. This project was carried out with extreme care and caution. The following discussion details the analyses that were made in order to evaluate whether or not to continue.

As with most field machinery diagnostic problems, there is always a combination of technical and economic factors to be considered. Clearly, the technical factors indicated that the balance state of the motor rotor was continuing changing. The two most probable causes were an ever increasing rotor bow due to uneven thermal heating of the motor rotor under load or a physical, continuing change in the mechanical balance state due to a moving or shifting mass that is a physical part of the rotor itself.

On 14 June, the initial thought was that the balance masses installed on 27 April had somehow come off of the rotor resulting in 1X vibration levels similar to the initial values from 27 April.

However, once the Wet Gas Compressor Train was shut down and the end bells removed from both ends of the motor, it was clearly evident that this was not the case. Both 118 gram masses, installed @ 300°, in both the A (outboard) and B (inboard) balance planes of the rotor, were still in place. Visual inspection of the motor rotor

from both ends revealed nothing unusual. Both journal bearings were inspected and found to be in acceptable condition.

The following data plots were acquired during the course of this project. Although acquired on different dates, they are representative of the response of the motor during the entire time period from 14 June through 14 July.

Figures 1 and 2 are transient shutdown data from 14 June. Figure 1 is a polar plot of the 1X (synchronous vibration) shutdown data from the inboard Y (45L) proximity probe while Figure 2 is a polar plot of the 1X shutdown data from the inboard X (45R) proximity probe.

In Figures 1 and 2, the rotor's first balance resonance is observed to occur slightly below operating speed at, approximately 1775 rpm, as indicated by the 90° phase lag relative to the low speed 1X vibration vector. It is interesting to note that at 1775 rpm, the 1X amplitude has not peaked. The difference between the speed where the maximum 1X amplitude would peak and the speed where the 90° phase shift occurred is attributed to: 1) damping in the system, and 2) longitudinal separation between the location of the residual unbalance (forcing function) and the longitudinal location of the proximity probes (measurement plane).

Figure 3 contains two bode plots of the filtered vibration response at twice synchronous (2X) frequency vs synchronous (1X) rotative speed as acquired on 14 July. The top portion of each bode plot depicts the change in 2X phase as a function of motor operating speed, Ω , while the bottom portion of each bode plot contains the 2X amplitude response as a function of Ω .

In both Plots A and B of Figure 3, the cursor is set at the peak of the 2X amplitude, which occurs at different frequencies in the two plots. In Plot A, the peak occurs at a motor operating speed of 1109 rpm (2X frequency = 2218

cpm), while in Plot B, the 2X peak occurs at a motor operating speed of 944 rpm (2X frequency = 1888 cpm).

The difference in the observed first balance resonance frequencies is typical of a *split resonance*, and is the result of stiffness asymmetry in the motor rotor / bearing / support system.

Although the data shown in Figure 3 is generated from the motor inboard end shaft relative proximity probes, which are mounted at an angular location of 45L and 45 R, the data has been manipulated in order to show how the data would appear from the perspective of a pair of “virtual transducers” located at 0 (top dead center, true vertical plane) and 90R (true horizontal plane) as opposed to the actual locations of 45L and 45R. This mathematical manipulation was performed in order to evaluate the stiffness asymmetry of the rotor / bearing system.

The data from this set of “virtual” transducers was created by mathematically transforming the actual vector data from two perpendicular probes at 45L and 45R via the following coordinate transform:

$$x = X \cos \theta + Y \sin \theta \quad (1)$$

$$y = -X \sin \theta + Y \cos \theta \quad (2)$$

By creating data from a set of “virtual” probes oriented in the true vertical and horizontal planes it is easier to evaluate the stiffness asymmetry in the rotor / bearing system.

By comparing the relative phase response between the outboard and inboard ends of the rotor it is clear that both the 1X and 2X vibration responses are *in phase* during the entire startup sequence. Consequently, the observed amplitude peaks represent a *split resonance* due to stiffness asymmetry between the true vertical and horizontal planes and are not the result of a separate first and second mode response.

Analyzing the data from the “virtual” transducers reveals that in actuality, the first balance resonance (critical speed) occurs over a frequency range from approximately 1400 through 3000 cpm with resonance peaks observed in the true horizontal plane near 18-1900 cpm and in the true vertical plane near at 2200 cpm.

POINT: INBOARD VERTICAL /45° Left 1X COMP SR: 0.416/261° 3.75/307° @1799 rpm
MACHINE: MOTOR
From 14JUN 12:27:47.3 To 14JUN 12:56:25.1 Shutdown

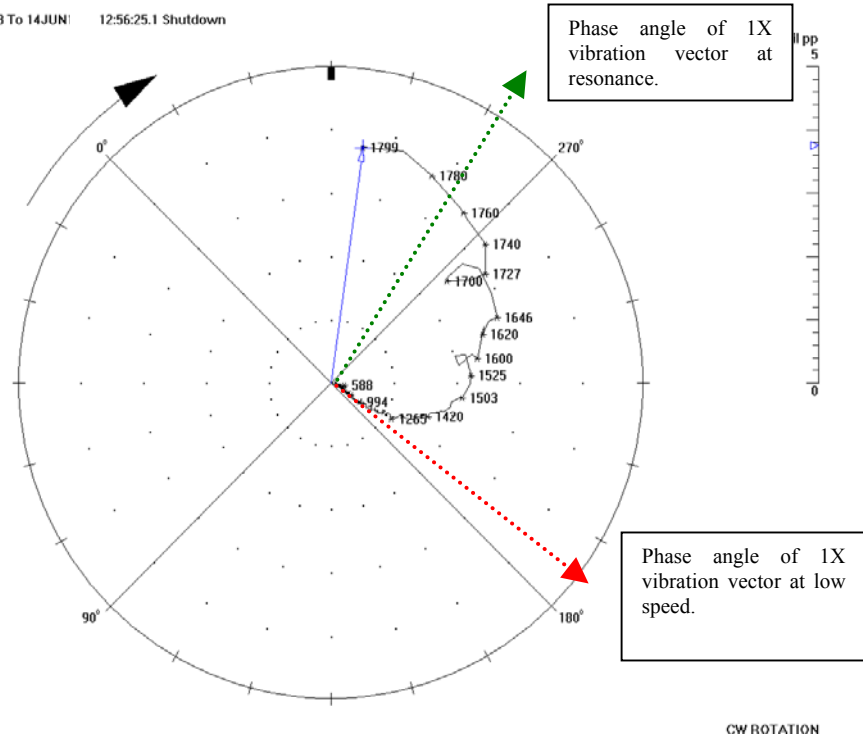


FIGURE 1

1X Shutdown Data – IB; 45L; Indicating Operating Speed Near First Balance Resonance Frequency

POINT: INBOARD HORIZONTAL /45° Right 1X COMP SR: 0.899/349° 1.62/74° @1799 rpm
MACHINE: MOTOR
From 14JUN 12:27:47.3 To 14JUN 12:56:25.1 Shutdown

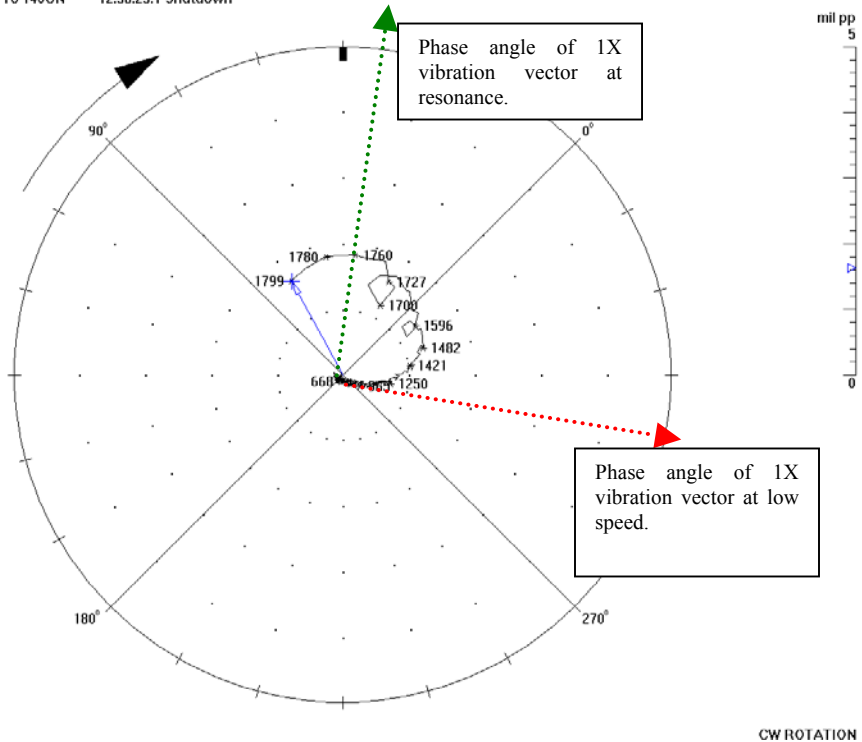


FIGURE 2

1X Shutdown Data – IB; 45R; Indicating Operating Speed Near First Balance Resonance Frequency

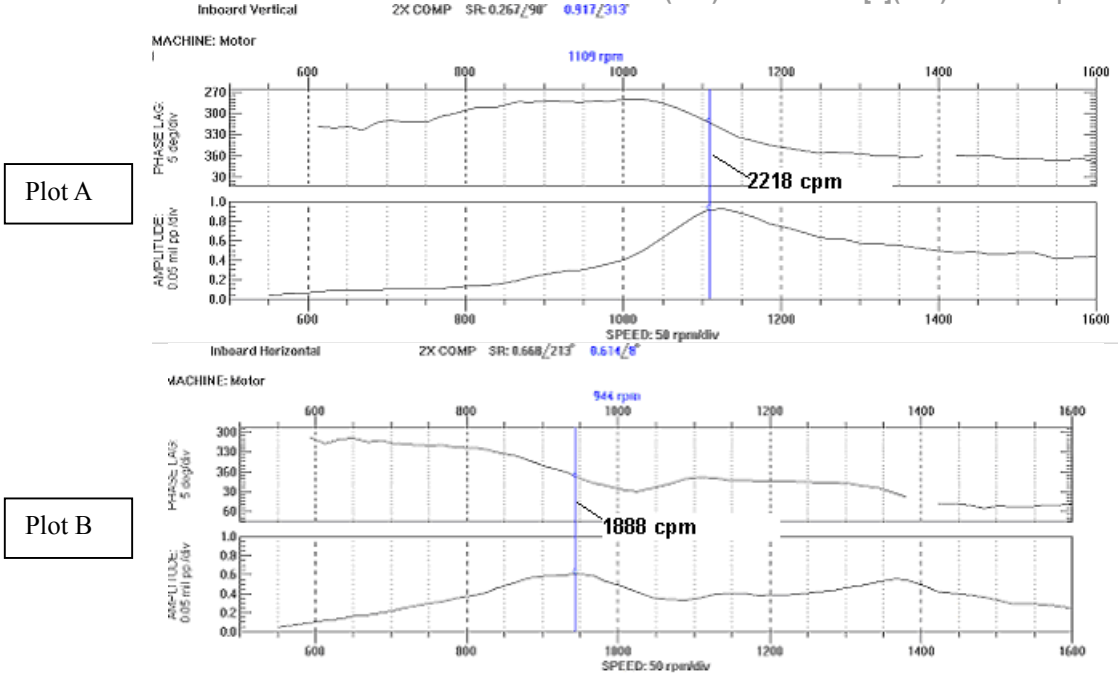


FIGURE 3
2X Data During Startup –Observed 1st Balance Resonance
1888 cpm (horizontal plane); 2218 cpm (vertical plane)

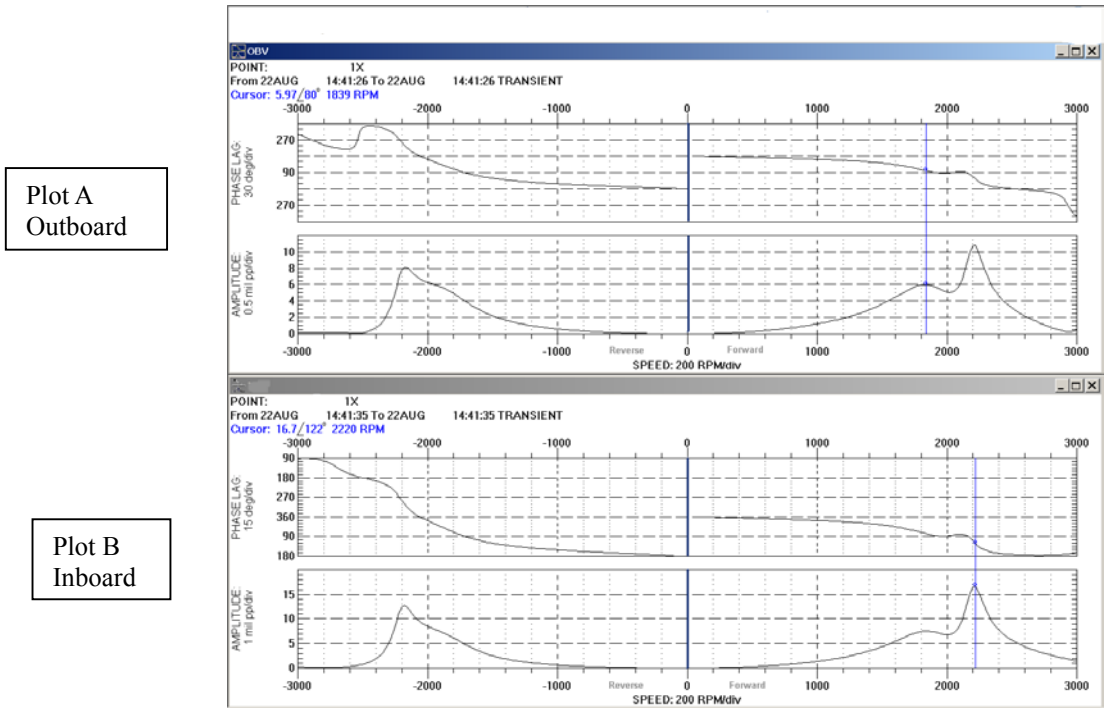


FIGURE 4
Finite Element Rotordynamic Model Data
Complex Filtered Forward / Reverse 1X Bode Plot from XY Orthogonal Transducers

Figure 4 contains two complex filtered bode plots depicting both the forward and reverse 1X components as generated from a finite element rotordynamic model of the motor rotor. Plot “A” is the complex filtered 1X bode plot from the outboard end of the rotor, while Plot “B” is the complex filtered 1X bode plot from the inboard end of the rotor. The rotordynamic model data closely agrees with the observed field data presented in Figure 3 revealing a split first balance resonance occurring near 1800 cpm (horizontal) and 2200 (vertical).

During the initial in situ field balancing on 27 April, a set of influence vectors, \vec{H} was calculated. The influence vector, $\vec{H}_{m,c}$, is used in balancing and defines the response of the rotor system in a given measurement plane, m , to a synchronous perturbation, e.g. centrifugal force, created in calibration plane c by the addition or removal of a calibration mass at a known radius at a known rotational speed.

The vector difference between the original 1X response and the 1X response resulting from the addition of the calibration mass is defined as the calibration response vector, \vec{C} , [*mils peak to peak (pp) $\angle \Phi^\circ$*]. The calibration mass and the angular location at which the calibration mass was installed (or removed) is known as the “weight add” vector, \vec{W} [*gram $\angle \Theta^\circ$*].

The influence vector is obtained by dividing the \vec{C} vector by the \vec{W} vector:

$$\vec{H} = \frac{C \text{ mil pp}}{W \text{ gram}} \angle \frac{\Phi^\circ}{\Theta^\circ} \quad (3)$$

The influence vector, \vec{H} , is a direct measurement of how the rotor system responds to a known 1X synchronous perturbation force that is created by the addition or removal of a known amount of mass at a fixed radius (12.5 inches for both balance planes of this motor) at a given rotational speed, Ω (1792 rpm for this motor).

The \vec{H} vector is assumed to remain constant for a given rotor system and a given set of operating conditions, e.g. load, temperature, speed, balance radius, etc. During field balancing, one is attempting to create a 1X vibration vector that is equal in magnitude and opposite in direction to the original 1X vibration vector that existed due to original unbalance state.

The \vec{H} vector allows one to directly calculate how much mass and at what physical location the mass should be added or removed in order to balance the rotor system.

During the data evaluation on 14 June, the influence vector from field balancing the motor rotor on 27 April was used in order to determine how much additional mass would be required to balance the rotor.

For this field balancing project, the motor was balanced in two planes, resulting in four influence vectors, two direct $\vec{H}_{1,1}$ and $\vec{H}_{2,2}$, and two longitudinal influence vectors, $\vec{H}_{1,2}$ and $\vec{H}_{2,1}$.

In the following discussion, vibration response data from the Inboard “Y” transducers (45° L) was utilized to calculate these influence vectors. (Refer to Figure 7 in the Appendix.) The inboard vertical influence vector is: $\vec{H}_{\text{INB VERT}} = 0.015 \text{ mil pp / gram @ } 99^\circ$. (Refer to Table 3 in the Appendix.)

For simplicity, in the following discussion, this single influence vector will be utilized. It should be noted, however, in actuality, all four influence vectors are utilized simultaneously in order to arrive at the required solution.

The physical meaning of the influence vector is that there will be a vibration response vector created with a magnitude of 0.015 mil pp for every gram of mass added. Furthermore, the vibration response vector will lag behind the location where the mass was added by 99°. The assumptions again are that the system is behaving as a linear spring and that the same set of operating conditions are in effect as were when the influence vectors were first calculated.

The phase lag of the influence vector is significant in and of itself in that the 99° lag angle also indicates that the rotor is operating very close to a balance resonance frequency. (Refer to Figure 1.) A lag angle of 90° would have implied operation at the resonance frequency. The 99° angle implies operation slightly above the resonance frequency at $\Omega = 1792$.

If we use the Inboard Vertical (45L) transducer data (refer to initial 14 June data – Table 1), the initial 1X vibration was 4.16 mil pp @ 302°. This is the *original* or \vec{O} vector. To balance the rotor, we need to create a vector equal in magnitude, but opposite in direction, e.g. $-\vec{O}$, or 4.16 mil pp @ 122°. The correct “weight add” vector can be determined by dividing $-\vec{O}$ by \vec{H} .

$$\begin{aligned} \vec{W}_{\text{correction}} &= \frac{4.16 \text{ mil pp}}{0.015 \text{ mil pp / gram}} @ \frac{122^\circ}{101^\circ} \quad (4) \\ &= 277 \text{ grams @ } 21^\circ \end{aligned}$$

The actual mass added on 14 June, determined via a simultaneous solution utilizing all four influence vectors, was 130 grams @ 15°, installed in both ends (balance

planes) of the motor rotor. The net effect was 260 grams @ 15°.

An additional item had to be considered in determining the required balance correction. Figure 5 documents the 1X response, as observed from the inboard proximity probe at 45L, during startup and the first 32 minutes of steady state data at 1792 rpm.

state vibration response occurred from 27 April through 14 July requiring five subsequent balance corrections on: 14 June, 21 June, 28 June, 5 July, and 14 July.

Figure 6 depicts the change in the 1X, as observed from the inboard proximity probe at 45L that occurred from 28 June through 5 July. This change in 1X vibration is very similar to the vector changes that occurred from:

- 27 April through 14 June
- 14 June through 21 June
- 21 June through 28 June
- 5 July through 14 July

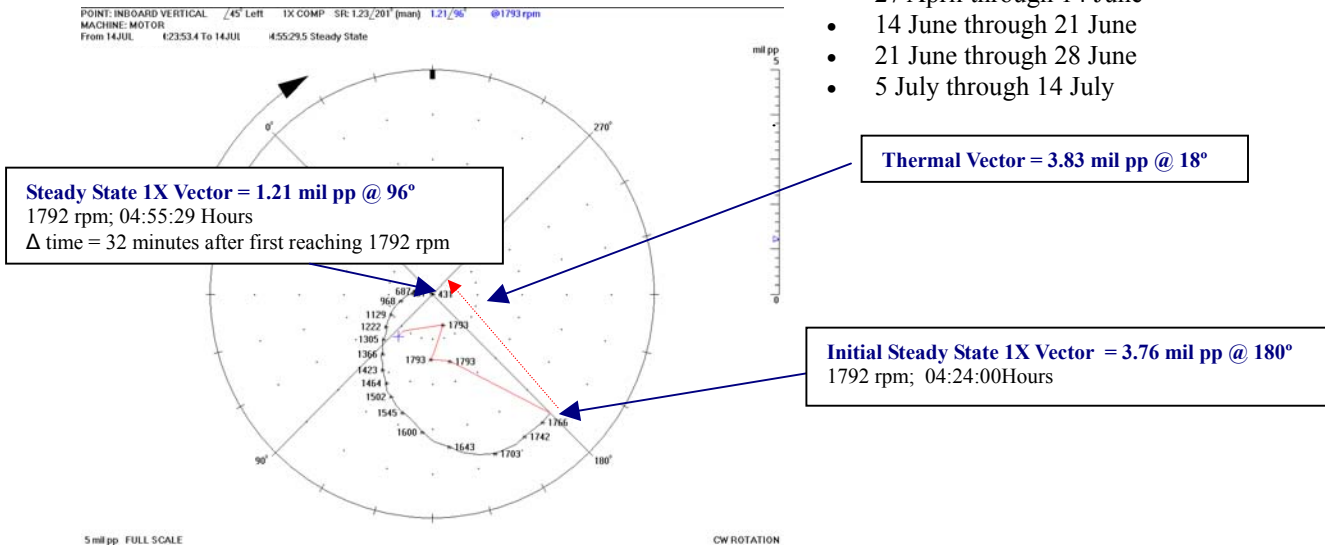


FIGURE 5

Thermal Vector - Startup & Initial Steady State

The initial 1X vibration response data at 1792 rpm is 3.76 mil pp @ 180°. Thirty two minutes later, the 1X response had changed to 1.21 mil pp @ 96°, a vector change of 3.83 mil pp @ 18°. This change in 1X response occurred under load and was consistent with a thermal load vector. Thermal load vectors result from uneven current flow through the rotor, resulting in a temperature differential and uneven axial expansion of the windings from on one side of the rotor as compared to the opposite side of the rotor. This uneven axial expansion bows the rotor, resulting in a change in the effective residual unbalance, and a corresponding change in the 1X vibration response data. This load related thermal vector was consistent and observable by all four proximity transducers throughout the eleven week period from 27 April through 14 July.

Once the motor rotor reached thermal equilibrium, initially the 1X steady state vibration response remained constant. However, over time, significant additional changes in the 1X steady state vibration response occurred.

MACHINERY DIAGNOSTIC ANALYSES

The motor had originally been balanced on 27 April. As shown in Table 2, significant changes in the 1X steady

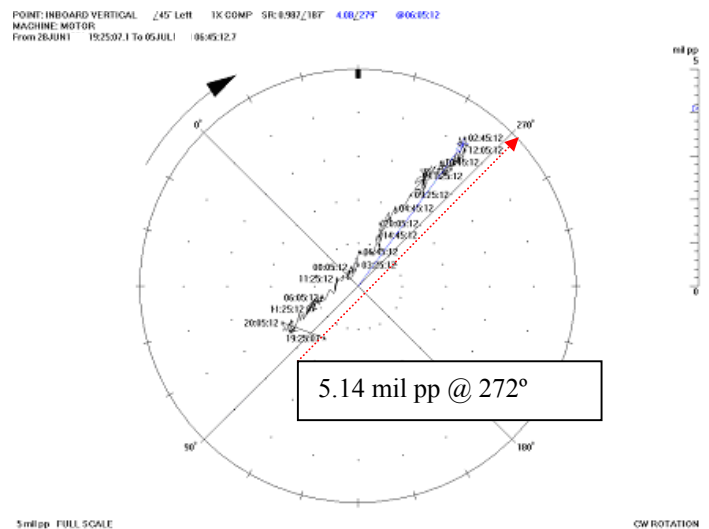


FIGURE 6

Δ 1X Vector Change from 28 June to 5 July = 5.14 mil pp @ 272°

What began initially as a field balancing project had now evolved into an investigation of a very serious machinery malfunction. In order to fully understand the

analysis process, it is necessary to review what the known facts were.

1. Motor initially field balanced on 27 April
2. INB_{VERT} influence vector from 27 April = 0.015 mil pp / gram @ 101°
3. From 27 April to 14 June, the 1X vibration vector change is 4 mil pp, requiring the motor to be field balanced a second time.
4. Balance masses installed on 27 April are still in place, confirming that the actual residual rotor unbalance mass had significantly increased.
5. Motor was balanced a second time, in one move, based on 27 April influence vector data.
6. Influence vectors calculated on 14 June were very similar to the original influence vectors of 27 April.
7. Changes were observed in the slow roll vector. From 14 June through 14 July, the total change was approximately 1 mil pp.
8. Rotor thermal bow was not changing. It remained constant as shown in Figure 5.
9. The *Synchronous Dynamic Stiffness* of the motor rotor was not changing.

The reciprocal of the \vec{H} vector has units of *mass / displacement*. If $1/\vec{H}$ is multiplied by $r\Omega^2$, and divided by the gravitational constant, g_c , the resulting expression will have units of *force divided by displacement* and is defined as the *Synchronous Dynamic Stiffness*, \vec{K}_{DS} .

$$\vec{K}_{DS} = \frac{1}{H} \times \frac{r\Omega^2}{0.5g_c} \begin{pmatrix} -\angle\Theta^\circ \\ -\angle\Phi^\circ \end{pmatrix} \quad (5)$$

or,

$$\vec{K}_{DS} = \frac{W}{C} \times \frac{r\Omega^2}{0.5g_c} -\angle(\Theta^\circ - \Phi^\circ) \quad (6)$$

Where:

$$\frac{Wr\Omega^2}{Cg_c} = \frac{\text{Force}}{\text{Displacement}}$$

r = calibration mass radius, 12.5 in

Ω = Rotational speed, 187.62 radians/second

g_c = Gravitational Constant;
386 (in - lb_m)/(lb_f - sec²),
or 1 (m - Kg)/(N - sec²)

$$1 \text{ lb}_m = 453.59 \text{ grams}$$

The factor of **0.5** is included in the denominator in order to convert from mils pp to mils peak. Dynamic Stiffness is defined as a peak force divided by a peak displacement, not peak to peak. Therefore, typical engineering units are expressed as either lb_f / in or N / m. Additionally, Dynamic Stiffness is derived based on phase lead angles. Because the phase angles are measured as phase lag angles, a negative sign is necessary as shown in Equation 5.

The gravitational constant is necessary in order to convert from mass units (grams) to force units (lb_f).

By using either Equation 5 or 6, the Synchronous Dynamic Stiffness can be calculated.

For example, if $\vec{H} = 0.015 \text{ mil pp / gram } \angle 99^\circ$ is used in Equation 5 as the influence vector, then a value of $335,085 \text{ lb}_f / \text{in } \angle 99^\circ$ is calculated as the average Synchronous Dynamic Stiffness. (Refer to Figure 8 in the Appendix.)

Therefore, it becomes readily apparent that although the influence vector and the synchronous dynamic stiffness vector are not direct reciprocals of each other, the reciprocal values are indeed related. This further leads one to the conclusion that if the influence vector increases, the synchronous dynamic stiffness decreases and vice versa..

Trending both the influence vector as well as the synchronous dynamic stiffness vector over time provides powerful insight as to whether or not modal properties of mass, damping, stiffness as well as bearing parameters such as the average circumferential velocity ratio, λ , are remaining constant or changing with time. Changing modal properties are strong indicators of a changing mechanical system.

By the time the motor rotor was field balanced for the third time on 21 June, it was very clear that:

1. The rotor's residual unbalance was increasing with time.
2. The rotor's balance condition was also being affected under load, by a repeatable, thermal bow.
3. The rotor's slow roll values were increasing.

Although the possibility of a serious shaft stiffness asymmetry malfunction, e.g. shaft crack, could not be ruled out, it was concluded that since the Synchronous Dynamic Stiffness and Influence Vectors were not changing with time, that the potential for a shaft crack was minimal.

The plant did not have a spare motor available to replace the motor in service. The spare motor was in the process of being repaired. The earliest that it could be

ready was early August. The decision was made to continue to operate the Wet Gas Compressor Train with increased diligence with respect to vibration monitoring in order to keep the refinery in production. It was also decided that the motor would be removed from service if the rate of change of the 1X vibration vector increased from its previously consistent level of 0.70 mil pp / day.

While the spare motor was being repaired, the motor did require additional balancing as summarized in Table 1.

During this time, Influence and Synchronous Dynamic Stiffness Vectors remained essentially constant. Additionally, the rate of change of the 1X vector did not increase. In actuality, during the last two weeks of July, the unit stabilized and the vibration levels remained constant.

The unit was removed from service during the first week of August and replaced with the repaired, spare motor.

Subsequent inspections revealed several problems with the motor rotor including sticking rotor coils, loose rotor coils, and migrating rotor iron.

CONCLUSION

Synchronous perturbation is an inherent part of every field balancing exercise. By synchronously perturbing the rotor system with a know centrifugal force, the response of the system to the synchronous perturbation force can be directly measured. From this information, both the Synchronous Dynamic Stiffness and Influence Vectors can be determined. Along with other direct and indirect (calculated) forms of machinery data, both the Synchronous Dynamic Stiffness and Influence Vectors are evaluated and trended over time.

Since the rotor response (vibration) is always equal to the summation of the dynamic forces that act on the rotor / bearing system divided by the complex dynamic stiffness of the system, it becomes apparent that an increase in rotor vibration may be due to:

1. An increase in the dynamic forces
2. A decrease in the complex dynamic stiffness
3. Both

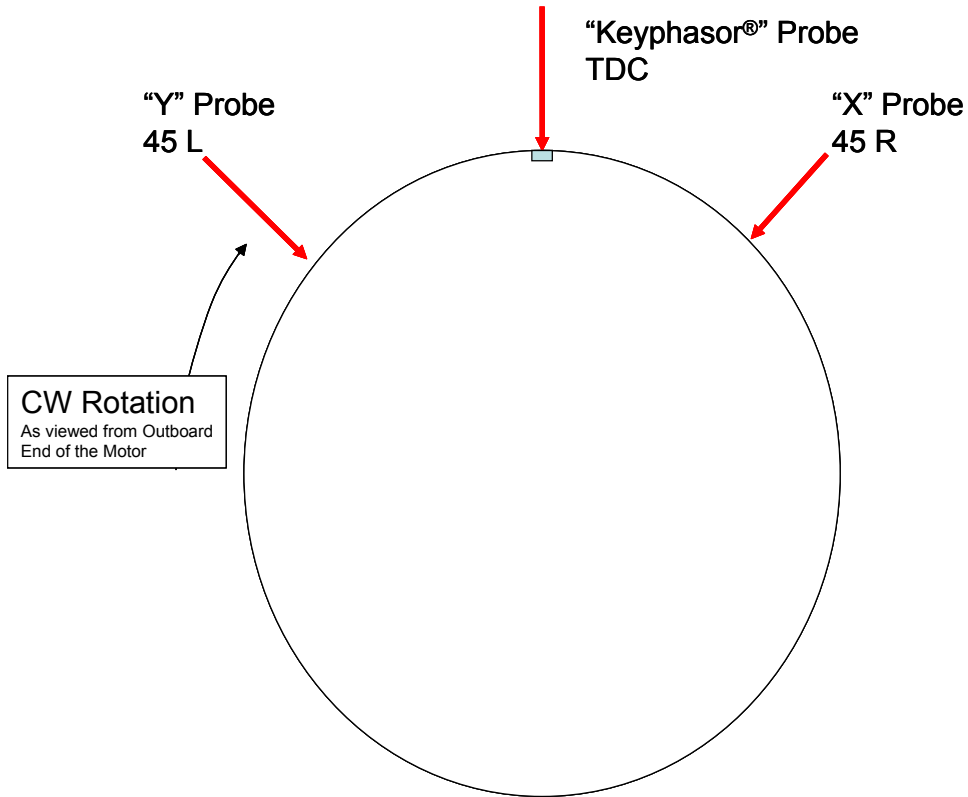
Analysis of field balancing data in order to determine the Influence and Synchronous Dynamic Stiffness properties of the rotor / bearing system provides powerful insight into the origin(s) of a change in rotor vibration.

operating risks are minimized and the proper machinery asset management is provided.

REFERENCES

1. "Historical and Future Views of Rotordynamics", Bently, Donald E., Orbit Magazine, September 1993
2. "Fundamentals of Rotating Machinery Diagnostics", Bently, Donald E., Hatch, Charles T., First Edition, Bently Pressurized Bearing Press, 2002.
3. "The Synchronous Amplification Factor, Split Resonances, and Virtual Probe Rotation", Hatch, Charles T., Orbit Magazine, June 1997
4. "Understanding and Using Dynamic Stiffness", Sabin, Steve, Orbit Magazine, 2nd Quarter, 2000
5. "Back to Basics – The Importance of Transient Data Analysis"; Thomas, Richard, Proceedings of the 18th Annual Meeting of the Vibration Institute; Hershey, PA; June 1994

APPENDIX



*Registered Trademark of Bently Nevada

FIGURE 7
Transducer Orientation

$$\vec{K}_{DS} = \left(\frac{1}{0.5\vec{H}} \right) \left(\frac{r\Omega^2}{g_c} \right)$$

$$\vec{K}_{DS} = \left(\frac{1}{0.5|H|} \right) \left(\frac{r\Omega^2}{g_c} \right) \left(\begin{array}{c} -\angle\Theta^\circ \\ \angle\Phi^\circ \end{array} \right)$$

$$\vec{K}_{DS} = \left(\frac{1}{0.5|H|} \right) \left(\frac{r\Omega^2}{g_c} \right) \angle -(\Theta^\circ - \Phi^\circ)$$

$$\vec{K}_{DS \text{ VERT}} = \left(\frac{1}{0.5(0.015 \text{ mil pp})} \right) \left(\frac{(12.5 \text{ in})(187.62 \text{ rad/sec})^2}{g_c} \right) \angle -(300^\circ - 39^\circ)$$

FIGURE 8
Calculation of Synchronous Dynamic Stiffness Vector

$$\overline{K}_{DS_{INB\ VERT}} = \left(\frac{1 \text{ gram}}{\left(\frac{0.5 \text{ mil}}{\text{mil pp}} \right) \left(\frac{0.015 \text{ mil pp}}{\text{mil pp}} \right)} \right) \left(\frac{(12.5 \text{ in}) \left(187.62 \frac{\text{rad}}{\text{sec}} \right)^2}{\frac{386 \text{ in} \cdot \text{lb}_m}{\text{lb}_f \cdot \text{sec}^2}} \right) \left(\frac{1000 \text{ mil}}{\text{in}} \right) \left(\frac{\text{lb}_m}{453.59 \text{ gram}} \right) \angle -(300^\circ - 39^\circ) =$$

$$335,085 \text{ lb}_f / \text{in} \angle 99^\circ$$

FIGURE 8a
Calculation of Synchronous Dynamic Stiffness Vector From the Influence Vector

OR, ALTERNATIVELY:

$$\vec{K}_{DS_{INB\ VERT}} = \frac{F}{C} \frac{1}{(0.5)} \begin{pmatrix} -\angle\Theta^\circ \\ \angle\Phi^\circ \end{pmatrix} = \frac{W}{C} \frac{(r\Omega^2)}{(0.5)} \angle -(\angle\Theta^\circ - \angle\Phi^\circ)$$

$$\vec{K}_{DS_{INB\ VERT}} =$$

$$\left[\frac{(236\ \text{grams} \angle 300^\circ)(12.5\ \text{in}) \left(187.62 \frac{\text{rad}}{\text{sec}}\right)^2}{(3.54\ \text{mil}\ \text{pp} \angle 39^\circ) \left(\frac{0.5\ \text{mil}}{\text{mil}\ \text{pp}}\right) \left(\frac{386\ \text{in}\text{-}\text{lb}_m}{\text{lb}_f\text{-}\text{sec}^2}\right)} \right] \left(\frac{1000\ \text{mil}}{\text{in}} \right) \left(\frac{1\ \text{lb}_m}{453.59\ \text{grams}} \right) \angle -(300^\circ - 39^\circ) =$$

$$335,085\ \text{lb}_f / \text{in} \angle 99^\circ$$

FIGURE 8b
Calculation of Synchronous Dynamic Stiffness Vector From Applied Force / Response

Balance Summary Data: April 27, 2005											
Run No.	Data Type	Date	BP	Mass Added (gms)	Mass Angle	+	-	Outboard 45L (vertical xducer) (mil pp @ Φ)	Outboard 45R (horz xducer) (mil pp @ Φ)	Inboard 45L (vertical xducer) (mil pp @ Φ)	Inboard 45R (horz xducer) (mil pp @ Φ)
1	Initial	27-Apr-05	1	118	300°	+		2.90 @ 225°	0.70 @ 346°	3.80 @ 211°	1.90 @ 325°
	Final	27-Apr-05	2	118	300°	+		0.30 @ 4°	0.50 @ 99°	0.60 @ 151°	0.40 @ 307°
mil pp	C Vector	27-Apr-05						3.13 @ 41°	1.00 @ 139°	3.54 @ 39°	1.52 @ 150°
mil pp/gram	H Vector	27-Apr-05						0.01326 @ 101°	0.00424 @ 109°	0.015 @ 99°	0.00644 @ 120°
Notes:								1) BP = Balance Plane; 1=Outboard; 2= Inboard 2) The "+" sign = mass added 3) The "-" sign = mass removed 4) All vibration data is shaft relative displacement data 5) Mass added at a 12.5 inch balance radius 6) Mass angle is referenced to the 45L (vertical) transducer with the Keyphasor transducer aligned with the once per turn hole. 7) Rotor rotation is CW as viewed from the outboard end			

TABLE 3